Int. J. Electrochem. Sci., 13 **(2018)** 8827 – 8837, doi: 10.20964/2018.09.27

International Journal of
ELECTROCHEMICAL
SCIENCE
www.electrochemsci.org

Performance of coating based on APTMS/GO/Epoxy composite for corrosion protection of steel

Chun Feng [1,2], *Lijuan Zhu* [1,2,*], *Yaqiong Cao* [1,2], *Yin Di* [3], *Zongxue Yu* [3,*], *Guhui Gao* [4]

[1] CNPC Tubular Goods Research Institute, Xi'an, 710077, China.
[2] State Key Laboratory for Performance and Structure Safety of Petroleum Tubular Goods and Equipment Materials, Xi'an, 710077, China.
[3] Southwest Petroleum University, School of Chemistry and Chemical Engineering, Chengdu, 610500, China.
[4] Redbud Innovation Institute, Baodi, Tianjin,301800, China.
[*]E-mail: zhulijuan1986@cnpc.com.cn, haiqingy@163.com

Received: 15 May 2018 / *Accepted:* 30 June 2018 / *Published:* 5 August 2018

This study reports a new strategy for providing epoxy coatings with enhanced barrier protection mechanisms. For this purpose, covalent modification of graphene oxide with 3-aminopropyltrimethoxysilane (APTMS-GO) made it easy to achieve a homogenous dispersion in an epoxy matrix. The stable dispersion of APTMS-GO was examined by TEM, SEM and XRD. Embedding a small percentage of well-dispersed APTMS-GO nanosheets (2.0 wt.%) in the epoxy coating remarkably improved anticorrosion performance. The electrochemical impedance spectroscopy (EIS), water contact angles and SEM revealed that the barrier performance of the epoxy coating was improved after addition of 2.0 wt.% APTMS-GO nanosheets to the epoxy coating sample, which was attributed to the well-dispersed APTMS-GO nanosheets in the epoxy matrix.

Keywords: Graphene oxide, 3-Aminopropyltrimethoxysilane, Epoxy, Corrosion resistant

1. INTRODUCTION

Oil and gas pipeline corrosion has a major impact on the cost of steel, the leaking of oil and gas, the environment and human safety[1]. To protect steel from corrosion, organic coatings was the most popular and cost-effective to control and mitigate the corrosion processes that take place on the interface of the metal and the coating[2, 3]. Additionally, the organic coatings protect the steel from corrosion through barrier mechanisms[4]. Epoxy coating has been widely used owing to its excellent adhesion properties, low shrinkage and price, outstanding chemical stability and corrosion resistance[5-7]. However, epoxy coating produces a multitude of cracks in the curing process that are

permeable to the corrosive electrolyte, which lead to the formation of corrosion products beneath the coating. Therefore, the epoxy coating can't provide long-term corrosion protection[8, 9]. In order to enhance epoxy coating performance, adding nanomaterials on the epoxy coating has been an excellent strategy[10, 11].

Among all the nanomaterials, the application of GO for prevention of metallic substrates from corrosion was reported [12-15] owing to its two-dimensional (2D) sheet structure that could enhance the barrier mechanisms of epoxy coating. However, GO has a pronounced tendency to aggregate owing to the high surface area and strong van der Waals force. This tendency leads GO to disperse in epoxy resin[16]. To improve the anticorrosion properties of the epoxy coating with added GO, the distribution of GO was required to increase. Additionally, an effective approach to improve the dispersity was functionalization of GO due to the many functional groups including hydroxyl, carbonyl, carboxyl and epoxide groups on the edge and the basal plane of GO nanosheets[17-19]. For instance, Zheng and coworkers [19] developed a new type of modified GO coating that retained the high dispersion of modified GO sheets in the polymer matrix. Additionally, the result revealed that the modified GO sheets significantly reinforced the corrosion protection property of epoxy coatings on carbon steel substrate. Ahmadi and coworkers [17] prepared silylated graphene oxide through a sol–gel route. The material could excellently disperse in the silane coating. The coating containing silanized graphene oxide showed superior corrosion protective performance compared to the unfilled silane coating.

Recently, 3-aminopropyltrimethoxysilane (APTMS), a silane coupling agents, has been widely used in polymers and resin coating systems as a dispersion promoters [20-22]. APTMS modification is a promising approach to improve the dispersity of GO in the epoxy coating.

In the present work, APTMS-GO nanosheets were fabricated through APTMS assisted linking to graphene oxide. After characterization of APTMS-GO by FT-IR, XRD, TGA and SEM analyses, 2 wt% APTMS-GO material [23-26] was incorporated into epoxy coating to prepare APTMS-GO/EP. The corrosion protection performance of the APTMS-GO/EP samples was examined by EIS and scratch tests. Finally, the APTMS-GO material could excellently disperse in the epoxy coating. The APTMS-GO/EP coatings provided more remarkable corrosion protection for metal than neat EP and GO/EP coatings.

2. EXPERIMENTAL

2.1. Materials

Natural graphite, H_2SO_4 (98%), H_2O_2, HCl, $KMnO_4$, $NaNO_3$, APTMS and acetone were purchased from Chengdu Kelong Chemical Reagent Factory (China). The EP emulsion (WSP-6101) and its curing agent used in this research were supplied by Bluestar Technology Wuxi Resin Factory. Deionized water (DI water) was produced by a water purification machine (UPC-III-40L, Ulupure).

2.2. Preparation of GO and APTMS-GO

GO was fabricated via a modified Hummers' method[27, 28], then, functionalized by APTMS[29, 30]. Briefly, a homogenous solution was formed by dispersing 0.1 g GO and 2.0 g APTMS in 50 g

anhydrous ethanol by ultrasonication, and then the mixture was heated to 70 ℃ in a water bath and refluxed for 4 h. Next, 10 g of distilled water was added drop wise into the mixture. Finally, the resulting solid was collected by centrifugation and washed with DI water and anhydrous ethanol several times. After drying in a vacuum oven at 60℃ overnight, APTMS-GO was obtained.

2.3. Preparation of composite EP coatings

EP coatings containing APTMS-GO (2wt%) were prepared by the following procedures. A certain amount of APTMS-GO was first added into an EP suspension followed by sonication for 5 min in an ice and water bath to form a homogeneous system before further use. Afterwards, the metal substrate (P110) was processed into a steel sheet. One part of the mixture was sprayed on the surface of the steel after mechanical stirring and ultrasonic oscillation. Then, the other part of mixture and the steel with mixture were cured in an oven for 1 h at 120℃, and for 2 h at 220℃. For comparison, other composite coatings containing GO and neat EP suspension were also prepared with similar procedure. Meanwhile, the cured EP coatings were denoted as APTMS-GO, GO/EP and EP, respectively. The EP mixture coated panels with a thickness of approximately 70μm.

2.4. Measurements

The morphologies of APTMS-GO and GO were studied by transmission electron microscopy (TEM, Tecnai G2 F20, FEI Company, USA). The morphologies of EP composite coatings were examined using scanning electron microscopy (SEM, JSM-7500F, JEOL, Tokyo, Japan). Fourier transform infrared (FT-IR) spectra were recorded with WQF-520 infrared spectrometer (Beijing Rayleigh Analytical Instrument Company, China) in the range of 4000-400 cm^{-1}. The crystal structure of samples was determined with a X'Pert Pro Diffractometer (PANalytical, The Netherlands) with a Cu Kα radiation source. The water contact angle (WCA) of electrodes was obtained with static contact angle meter (XED-SPJ, Peking Hako Experimental Instrument Plant, China).

Electrochemical impedance spectroscopy (EIS) measurements were performed using the frequency range of 10^{-1}-10^{4} Hz with an amplitude sinusoidal voltage of 10 mV using an electrochemical workstation (Shanghai Brilliance Instruments Limited Company, China). The EP-coated steel coupon served as the working electrode, while a platinum grid and a saturated calomel electrode (SCE) were used as the counter and the reference electrode, respectively. Measurements were carried out in 3.5% NaCl solution. ZSimpWin software was used for fitting the EIS data.

3. RESULTS AND DISCUSSION

3.1. Structure and morphology of APTMS-GO

TEM was employed to compare and explore the structure and morphology of GO and APTMS-GO, as shown in Fig. 1. GO exhibited a randomly folded structure (Fig. 1a), which was consistent with

a previous study[29]. After modification, the APTMS-GO still retained a wrinkled morphology (Fig. 1b). Notably, the multilayered sheets of GO with stacked structure, shown in Fig. 1a, was unfavorable to disperse within the polymer matrix. For APTMS-GO, one could see that GO sheets exhibited thin-layered sheets with a loosened state and maintained their two dimensional sheet morphology (Fig. 1b). According to a previous report [31], the thin-layered structure of the nanofiller had a tendency to achieve a uniform distribution within the polymer compared with the multilayered structure. The structures of GO and APTMS-GO were further investigated by XRD.

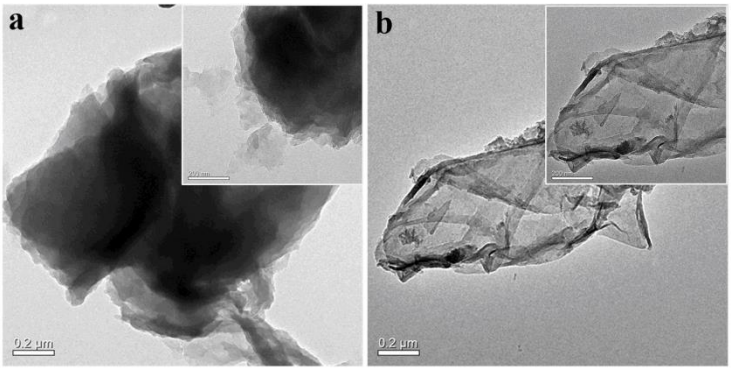

Figure 1. TEM images of (a) GO, (b) APTMS-GO.

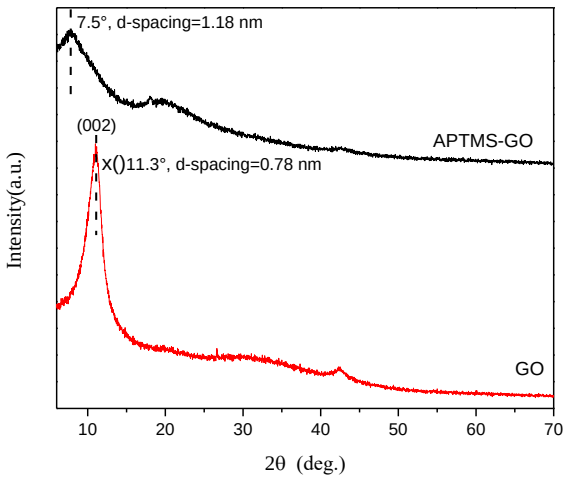

Figure 2. XRD pattern of GO and APTMS-GO

Fig. 2 depicts the XRD pattern of GO and APTMS-GO. For the GO sample, the peak at 2θ=11.3°, corresponding to a d-spacing of 0.78 nm, related to the (002) diffraction peak of GO sheets[29]. After modification with APTMS, a broad and weak peak at 2θ=7.5°, corresponding to a d-spacing of 1.18 nm, appeared in the curve of APTMS-GO. Comparing the pattern of APTMS-GO with GO, the increase of d-spacing indicated the stacked sheets have been loosened due to the intercalation of the silane molecules, which was in accordance with the result obtained by TEM analysis.

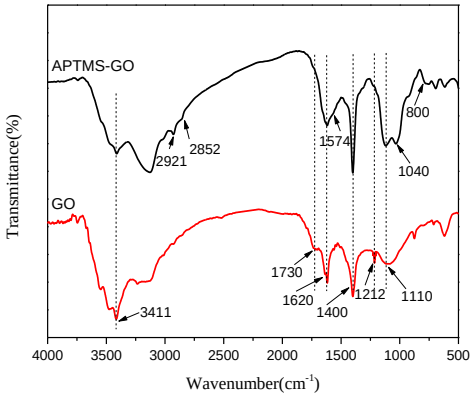

Figure 3. FT-IR spectra of GO and APTMS-GO

The FTIR spectra of GO and APTMS-GO are shown in Fig. 3. The characteristic absorption peaks of GO at 3411 cm^{-1} (–OH), 1730 cm^{-1} (C=O), 1212 cm^{-1} (C–O), and 1110 cm^{-1} (C–O–C), reveal the oxygenousfunctional groups consisting of hydroxyl, carboxylic and epoxy group on GO sheets[32, 33]. The peaks at 1620 and 1400 cm^{-1}were associated with the C=C and=C–H band[34]. After modification, some new absorption bands were observed in the spectrum of the APTMS-GO. The peaks approximately 2921 and 2852 cm^{-1} represented C–H bonding. More importantly, the absorption peak at 1040 cm^{-1} assigned to Si−O−C stretch vibration, and the appearance of the band at 1574 cm^{-1} provided evidence for APTMS grafted on the GO[31]. Combined with SEM, TEM and XRD analysis, these results confirmed the coverage of APTMS on the GO surface.

3.2. Dispersion of APTMS-GO in EP

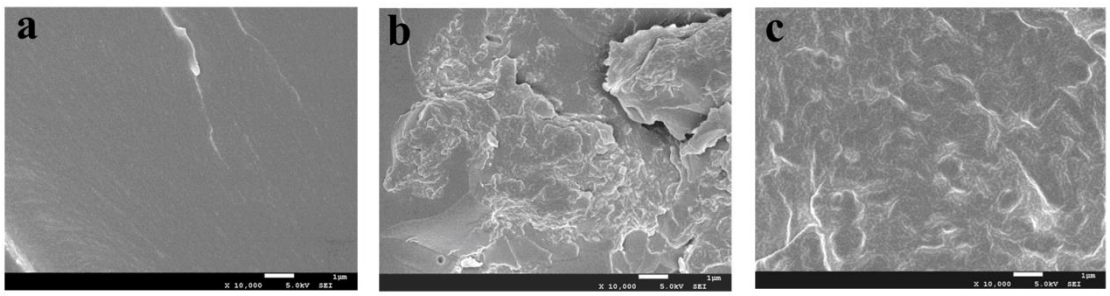

Figure 4. SEM images of fracture surfaces of (a) EP, (b) GO/EP, (c) APTMS-GO/EP

Fig. 4 shows the SEM images of the fractured surfaces of neat EP, GO/EP and APTMS-GO/EP. Fig. 4a shows a clean fracture surface of the EP, implying the brittle nature of EP. In contrast to the GO/EP and APTMS-GO/EP, the EP showed rougher fractured morphology, representing higher roughness. In addition, GO sheets were unevenly dispersed in the EP matrix with multilayer structure (Fig. 4b), while functionalized GO was uniformly distributed in EP matrix with thin-layered morphology (Fig. 4c). In contrast to the large-scale aggregates of GO within EP, APTMS-GO exhibited no aggregates dispersed in the EP, which was attributed to the fact that covalent links

between the amino groups of APTMS-GO and EP had formed, and there was no exact boundary between each other. Herein, APTMS-GO exhibited excellent distribution and compatibility within the EP matrix.

3.3. Corrosion resistance of EP coatings

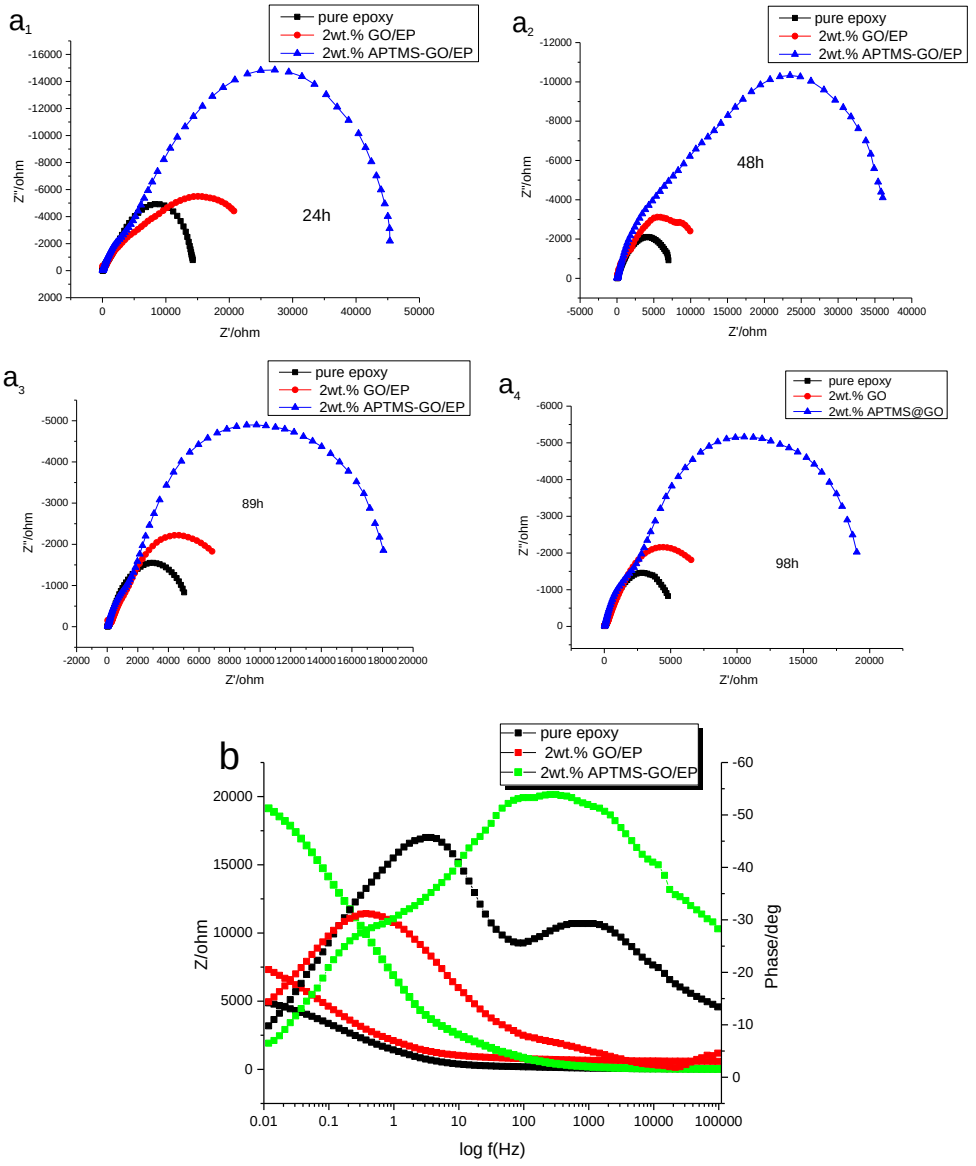

Figure 5. (a) Nyquist plots of all coatings after 24h, 48h, 89h and 96h of immersion in 3.5% NaCl electrolyte. (b) Bode plots of neat EP, GO/EP (2wt. %), and APTMS-GO/EP (2wt. %) after 96h.

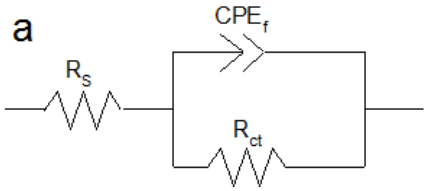

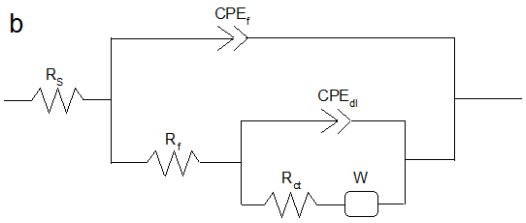

Figure 6. The equivalent circuit of sample

The anticorrosion performance of all coatings including pure EP, GO/EP (2wt. %) and APTMS-GO/EP (2wt. %) coatings were compared and investigated by electrochemical impedance spectroscopy (EIS) measurements. Before the electrochemical test, the open circuit potential (OCP) of samples was steady in 3.5% NaCl solution in that its value changed only 0.1 mV. Their Nyquist plot was respectively shown in Fig. 5 a_1-a_4 after 24 h, 48 h, 89 h and 96 h of immersion in 3.5% NaCl aqueous solution, Fig. 5b is the Bode plot of these coating after soaking for 96 h. According to these pictures (Fig. 5a) that denoted the impedance spectra of the pure EP, GO/EP (2wt. %) and APTMS-GO/EP (2wt. %) coatings at different immersion times, the radius of impedance arc of the APTMS-GO/EP coating was greater than pure EP and GO/EP after the same immersion time in 3.5% NaCl electrolyte. Therefore, the APTMS-GO/EP coating had the greatest the impedance modulus. The Bode plot of the three coatings (Fig. 5b) shows that the neat EP coating had a two-time constant and other coating had only one when they remained for 96 h in the 3.5% NaCl solution.

ZSimpwin software was used to fit the EIS data to realize the corrosion process and obtain the equivalent electric circuit in good agreement with the electrochemical test (Fig. 6). The constant phase element of the fitted results was as follow: R_s, CPE_f, R_f , R_{ct}, CPE_{dl}, and W respectively corresponding to the electrolyte resistance, the coating capacitance, the coating resistance, the charge transfer resistance, the double layer capacitance and the Warburg resistance.

Many reports demonstrated the corrosive process consisted of two stages. First, the aggressive medium passed the micropores into the coating, and did not contact with the interface of metal/coating, which corresponded to the equivalent electric circuit of Fig. 6a. Second, the corrosive reaction with the steel would take place at the interface, and produce the corrosion products. This stage is the key period to judge if the coating had a corrosion prevention effect and was well-matched with the equivalent electric circuit in Fig. 6b. In general, as time increased, the anticorrosion property of coating weakened.

Through numerous studies[35, 36, 18, 37] that demonstrated the impedance of the sample corresponded to the corrosion, and the above description, the APTMS-GO/EP coating was able to substantially boost the anticorrosion performance of the EP and GO/EP coating. The causes were as follows: the APTMS-GO/EP coating had the greatest impedance modulus after the same immersion time in 3.5% NaCl electrolyte, and the neat EP did little, if anything to protect the metal at 96 h, resulting in the appearance of two-time constant on the Bode plot (Fig. 5b) and was relevant to the Warburg resistance on the equivalent electric circuit (Fig. 6b). Moreover, the mechanism was due to the barrier effect of the GO and increasing the dispersion of GO by the APTMS (Fig. 4c).

Consequently, the EP coating with added APTMS-GO was able to substantially boost the anticorrosion performance over that of the EP and GO/EP coatings.

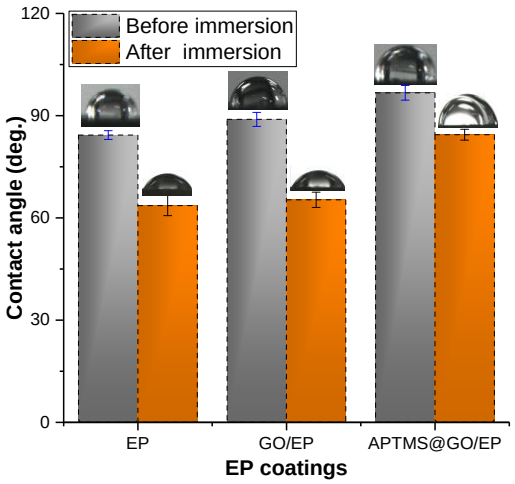

Figure 7. The water contact angles and typical images of water droplets on the EP coatings corresponded to EP, GO/EP and APTMS-GO/EP before and after 15 days of immersion in 3.5% NaCl electrolyte.

Water permeability resistance of coatings was closely associated with coating protective performance on steel[38]. The water contact angles (WCAs) and typical images of water droplets on EP, GO/EP and APTMS-GO/EP coatings are shown in Fig. 7. Before immersion, the contact angle of neat EP was 84.3°, which presented hydrophilic properties. When GO and APTMS-GO/EP were incorporated into the EP matrix, the WCAs of corresponding coatings' surface generally showed increases (~88.9° and ~96.7°). Interestingly, APTMS-GO/EP wholly exhibited hydrophobicity. It was noted that the hydrophobic surface could extend the initial soaking stage ascribed to hydrophobic properties and increase the wettability time of coatings' surface to protect the steel[39, 40]. After 15 days of immersion, the WCAs of EP, GO/EP and APTMS-GO/EP coatings decreased obviously (corresponding to ~63.6°, ~65.3° and ~84.4°, respectively), revealing that the anticorrosion performance of EP coatings was degraded gradually with the extension of immersion time. Remarkable, the WCA of the APTMS-GO/EP still remained at a maximum, reflecting the surface of APTMS-GO/EP reduced the corrosive medium (electrolyte solution) contacting with the organic coating to protect steel from corrosion for a relative long time compared other EP coatings. Namely, APTMS-GO/EP had a better anticorrosion performance among the three coatings, which can be validated in the monitoring of coatings' morphologies measurement.

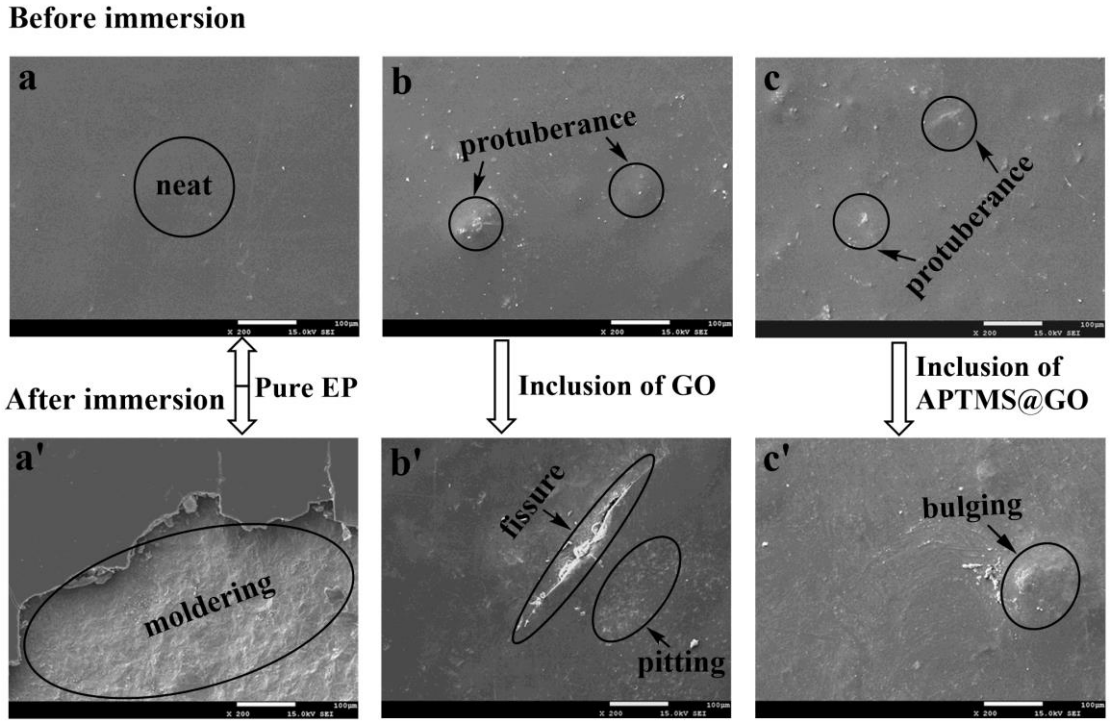

Figure 8. SEM images of electrodes about pure EP (a, a'), GO/EP (b, b') and APTMS-GO/EP (c, c') immersed in 3.5% NaCl electrolyte; a-c and a'-c' corresponded to before and after soaking for 15 days.

Fig.8 a-c and a'-c' present SEM images of electrodes with pure EP, GO/EP and APTMS-GO/EP before and after soaking for 15 days of immersion in 3.5% NaCl electrolyte, respectively. A neat and clean morphology was initially observed on the surface of the coated pure EP electrode (Fig. 8a), which was then seriously corroded, and a large area of moldering phenomenon appeared in the surface of the electrode (Fig. 8a'), indicating the poor corrosion resistance after 15 days. Protuberances appeared in coated GO/EP and APTMS-GO/EP surface of steel (Fig. 8b), owing to the incorporation of nanofillers to EP. The fissure and pitting were observed in the electrode surface of GO/EP (Fig. 8b') after soaking. Interestingly, a negligible change was presented in-coated APTMS-GO/EP steel with roughening and bulging at the surface of electrode (Fig. 8c') after soaking. Apparently, the morphological change of the electrode was related to the corrosion resistant performance. The inconspicuous morphological change of APTMS-GO/EP electrode exhibited an outstanding corrosion protective performance on steel compared with the GO/EP and EP electrode. This conclusion was consistent with electrochemical measurement and WCAs data.

4. CONCLUSIONS

The structure and morphology of the APTMS-GO materials were characterized by TEM, XRD and FTIR to certify the high specific surface and superior barrier effect. Then, the APTMS-GO/EP coating was prepared and applied for protection of metals from the corrosion medium. The APTMS-

GO/EP coating had favorable anticorrosive propertiesy, which was testified by the electrochemical impedance spectroscopy (EIS), water permeability resistance of coatings and the SEM images of electrodes in 3.5% NaCl electrolyte. APTMS-GO was well-dispersed in EP. In sum, the new EP coating containing the APTMS-GO material had excellent corrosion resistance.

ACKNOWLEDGEMENT
This work received the support of the Basic research and Strategic reserve Technology Fund of CNPC (2017Z-04).

References

1. A.Inoue, *Acta. Mater*., 48 (2000) 279.
2. Z. Wang, E. Han, F. Liu, Z. Qian, L. Zhu, *J. Mater. Sci. Technol*., 30 (2014) 1036.
3. H. Shi, F. Liu, E.H. Han, *J. Mater. Sci. Technol*., 31 (2015) 512.
4. S. González, F. Cáceres, V. Fox, R.M. Souto, *Prog. Org. Coat.*, 46 (2003) 317.
5. J. Yu, R. Huo, C. Wu, X. Wu, G. Wang, P. Jiang, *Macromol. Res*., 20 (2012) 816.
6. Z. Karami, F. Nademi, M.J. Zohuriaan‐Mehr, A. Rostami, *J. Mater. Sci. Technol*., 134 (2017).
7. R. Li, H. Zhang, C. Zhou, B. Zhang, Y. Chen, H. Zou, M. Liang, *J. Mater. Sci. Technol*., 134 (2017) 45272.
8. X. Shi, T.A. Nguyen, Z. Suo, Y. Liu, R. Avci, *Surf. Coat. Tech*., 204 (2009) 237.
9. H. Feng, X. Wang, D. Wu, *Ind. Eng. Chem. Res*., 52 (2013) 10160.
10. S.K. Kumar, M. Castro, A. Saiter, L. Delbreilh, J.F. Feller, S. Thomas, Y. Grohens, *Mater. Lett.*, 96 (2013) 109.
11. M. Zabet, S. Moradian, Z. Ranjbar, N. Zanganeh, *J. Coat. Technol. Res*., 13 (2015) 191.
12. M. Rajabi, G.R. Rashed, D. Zaarei, *Corrosion Engineering Science & Technology*, 50 (2014) 174.
13. A.Y.H. Alhumade, *Express. Polym. Lett.*, 10 (2016) 1034.
14. S. Pourhashem, M.R. Vaezi, A. Rashidi, M.R. Bagherzadeh, *Prog. Org. Coat*., 111 (2017) 47.
15. S. Zhang, J. Yang, B. Chen, S. Guo, J. Li, C. Li, *Surf. Coat. Tech*., 326 (2017).
16. L.C. Tang, Y.J. Wan, D. Yan, Y.B. Pei, L. Zhao, Y.B. Li, L.B. Wu, J.X. Jiang, G.Q. Lai, *Carbon*, 60 (2013) 16.
17. A. Ahmadi, B. Ramezanzadeh, M. Mahdavian, *Rsc. Adv*., 6 (2016) 54102.
18. Y. Ma, H. Di, Z. Yu, L. Liang, L. Liang, P. Yang, Y. Zhang, D. Yin, *Appl. Surf. Sci*., 360 (2016) 936.
19. H. Zheng, Y. Shao, Y. Wang, G. Meng, B. Liu, *Corros. Sci.*, (2017).
20. M. Lin, F. Chu, A. Guyot, J.L. Putaux, E. Bourgeat-Lami, *Polymer*, 46 (2005) 1331.
21. M. Behzadnasab, S.M. Mirabedini, K. Kabiri, S. Jamali, *Corros. Sci*., 53 (2011) 89.
22. K.K. Pohaku Mitchell, A. Liberman, A.C. Kummel, W.C. Trogler, *J. Am. Chem. Soc*., 134 (2012) 13997.
23. H. Yi, C. Chen, F. Zhong, Z. Xu, *High. Perform. Polym*., 26 (2013) 255.
24. H. Di, Z. Yu, Y. Ma, Y. Pan, H. Shi, L. Lv, F. Li, C. Wang, T. Long, Y. He, *Polym. Advan. Technol.*, 27 (2016) 915.
25. Y. Ma, H. Di, Z. Yu, L. Liang, L. Lv, Y. Pan, Y. Zhang, D. Yin, *Appl. Surf. Sci*., 360 (2016) 936.
26. Z. Yu, L. Lv, Y. Ma, H. Di, Y. He, *Rsc. Adv*., 6 (2016) 18217.
27. Z. Yu, H. Di, Y. Ma, Y. He, L. Liang, L. Lv, X. Ran, Y. Pan, Z. Luo, *Surf. Coat. Tech*., 276 (2015) 471.
28. J. Si, Y. Liu, S. Chang, D. Wu, B. Tian, J. Zhang, *Res. Chem. Intermediat*., (2016) 1.
29. Z. Li, R. Wang, R.J. Young, L. Deng, F. Yang, L. Hao, W. Jiao, W. Liu, *Polymer*, 54 (2013) 6437.

30. W. Sun, L. Wang, T. Wu, M. Wang, Z. Yang, Y. Pan, G. Liu, *Chem. Mater*., 27 (2015) 2367.
31. M. Kim, D.Y. Kim, Y. Kang, O.O. Park, *Rsc. Adv*., 5 (2014) 3299.
32. K.S. Kim, I.Y. Jeon, S.N. Ahn, Y.D. Kwon, J.B. Baek, *J. Mater. Chem*., 21 (2011) 7337.
33. S. Hou, S. Su, M.L. Kasner, P. Shah, K. Patel, C.J. Madarang, *Chem. Phys. Lett*., 501 (2012) 68.
34. J. Forniés, A. Martín, L. Martín, B. Menjón, H.A. Kalamarides, L.F. Rhodes, C.S. Day, V.W. Day, *Chem-Eur. J.*, 8 (2002) 4925.
35. H. Yi, C. Chen, F. Zhong, Z. Xu, *High Perform. Polym*., 26 (2014) 255.
36. Y. He, Y. Fan, P. Luo, Q. Yang, *Russ. J. Appl. Chem+*., 88 (2015) 962.
37. Z. Yu, L. Lv, Y. Ma, H. Di, Y. He, *Rsc. Adv*., 6 (2016) 18217.
38. C. Zhu, X. Rui, J. Xue, L. Song, *Electrochim. Acta*., 56 (2011) 5828.
39. S. Shreepathi, S.M. Naik, M.R. Vattipalli, *J. Coat. Technol. Res*., 9 (2012) 411.
40. K.C. Chang, M.H. Hsu, H.I. Lu, M.C. Lai, P.J. Liu, C.H. Hsu, W.F. Ji, T.L. Chuang, Y. Wei, J.M. Yeh, *Carbon*, 82 (2015) 611